ELSEVIER

Journal of Wind Engineering
and Industrial Aerodynamics 69–71 (1997) 657–669

JOURNAL OF
wind engineering
AND
industrial
aerodynamics

Analysis interpretation modeling and simulation of unsteady wind and pressure data

K. Gurley, A. Kareem*

NatHaz Modelling Laboratory, Department of Civil Engineering and Geological Sciences, University of Notre Dame, 163 Fitzpatrick, Notre Dame, IN 46556, USA

Abstract

This paper addresses the analysis, modeling and simulation of measured full-scale wind pressure and velocity data. The records exhibit both non-Gaussian and non-stationary features, and are ideal for the application of a number of contemporary methods for handling the types of problems associated with these characteristics. Modeling the probability density function (pdf) of non-Gaussian pressure is first addressed, followed by the simulation of pressure data through new static transformation techniques. The non-stationary portion of the pressure data is isolated and decomposed into a set of localized basis functions using wavelet transform techniques.Wavelet analysis is used for the identification of energy flux in time and for simulation of the non-stationary wind velocity records.

Keywords: Random processes; Non-Gaussian; Probability; Wavelets; Wind; Non-stationary; Simulation; Aerodynamics

1. Introduction

The assurance of the safety and reliability of structures subjected to environmental loads requires the consideration of their extreme response. Of particular interest is the prediction of structural response due to severe loads, where the statistical description differs significantly from Gaussian, e.g. wind pressure fluctuations on building envelopes, and non-linear structural response. Highly non-Gaussian localized wind loads are often encountered on structures, particularly in separated flow regions, which may lead to increased expected damage on glass panels and higher fatigue effects on building envelope and cladding components. This paper presents methods applicable for the prediction of structural behavior under non-Gaussian loading, with emphasis on atmospheric wind loading. Some approaches to probability density function (pdf)

* Corresponding author.

PII S0167-6105(97)00195-5

modeling are first discussed, including new models based on existing maximum entropy and Hermite transformation formulations. Next, we present a new technique to simulate non-Gaussian wind and pressure fields to predict non-linear structural response to non-Gaussian wind loads for time domain integration schemes. Finally, wavelet analysis is used as a tool for both analysis and simulation of structural response and non-stationary wind data.

2. Probability density function modeling

In the context of reliability analysis and fatigue, an accurate probabilistic representation of input forces and structural response in the extreme region is essential for meaningful results. The log-normal distribution has been used in the literature to model pressure data as the tail of the distribution is higher than that of the normal distribution. This often provides values close to the observations, but may fail to predict the occurrence of values far from the mean. Two approaches to modeling the pdf of non-Gaussian pressure records concerning separated regions are considered here. Models based on maximum entropy and a Hermite transformation approach are applied to a pressure record utilizing measured moment values from the data to determine model parameters. Further motivation for improved pdf modeling will be presented in Section 3.

2.1. Maximum entropy method

The maximum entropy method (MEM) maximizes the Shannon entropy functional subject to constraints in the form of moment information. The pdf which maximizes the entropy functional is the least biased estimate for the given moment information. The Lagrange multiplier method is applied to solve this variational problem, and provides the joint pdf of higher-order systems directly. A brief outline of MEM is presented here. Complete details can be found in Refs. [1, 2].

The available information for a process $\boldsymbol{y}(t)$ can be expressed as joint moments

$$E[y_1^{r_1}y_2^{r_2}\dots y_n^{r_n}] = \int\cdots\int y_1^{r_1}y_2^{r_2}\dots y_n^{r_n}p(\boldsymbol{y})\,\mathrm{d}\boldsymbol{y} = m_{r_1\dots r_n}, \quad (1)$$

where n is the order of the system, $r_i = 0,1,2,\dots,M$, where M is the maximum order or correlation moment, $p(\boldsymbol{y})$ is the joint pdf, and $m_{r_1\dots r_n}$ is the value of the joint moment. The preceding integral is n-fold. One possible pdf of the process $\boldsymbol{y}(t)$ maximizes the entropy functional,

$$H = -\int p(\boldsymbol{y})\ln(p(\boldsymbol{y}))\,\mathrm{d}\boldsymbol{y}, \quad (2)$$

subject to constraints from the moment information.

After application of the Lagrange multiplier method, the resulting description of $p(\boldsymbol{y})$ for an n-dimensional case is

$$p(\boldsymbol{y}) = \exp(-\lambda_0 - 1)\exp\left(-\sum_{r_1 + \cdots + r_n}^{M} \lambda_{r_1 \cdots r_n} y_1^{r_1} \cdots y_n^{r_n}\right). \tag{3}$$

Substitution of Eq. (3) into the moment constraints and an additional normalization constraint $\int p(\boldsymbol{y})\mathrm{d}\boldsymbol{y} = 1$ gives the following system of equations:

$$\int y_1^{r_1} \cdots y_n^{r_n} \exp\left(-\sum_{r_1 + \cdots + r_n}^{M} \lambda_{r_1 \cdots r_n} y_1^{r_1} \cdots y_n^{r_n}\right)\mathrm{d}\boldsymbol{y} = m_{r_1 \cdots r_n} \tag{4}$$

and

$$\int \exp\left(-\sum_{r_1 + \cdots + r_n}^{M} \lambda_{r_1 \cdots r_n} y_1^{r_1} \cdots y_n^{r_n}\right)\mathrm{d}\boldsymbol{y} = \exp(\lambda_0 + 1). \tag{5}$$

This system of non-linear integral equations is solved numerically for $\lambda_{r_1 \cdots r_n}$, and the results yield the least biased estimate of the system joint pdf under the given moment constraints using Eq. (3). The moment information which constrains the maximum entropy functional may be in the form of moment equations rather than moment values as presented above. Details are omitted here; interested readers may refer to Ref. [1].

The MEM pdf based on higher-order moment constraints is expressed as the exponential of a polynomial, typically of fourth order or higher. In many cases, this leads to poor estimates in the tail region where the higher-order terms dominate. When data records are available, the tail limitations may be alleviated if one extracts process information other than higher-order moment values. This study makes use of the fractional and negative integer moments as constraint information for non-Gaussian pressure data, and shows significant improvement over the use of the first four moments as constraints. MEM using constraints in the form of the first four moments and negative integer moments are referred to herein as MEM I and MEM II, respectively. An example follows the next section.

2.2. Hermite moment method

This approach is based on a functional transformation of a standardized non-Gaussian process, $x(t)$, to a standard Gaussian process, $u(t)$ (e.g. Ref. [3])

$$x(t) = (X(t) - \bar{X})/\sigma_X = g[u(t)]. \tag{6}$$

A cubic model of $g(u)$ offers a convenient and fairly accurate representation [4]. Accordingly, the pdf of $x(t)$ is given by Refs. [3, 4]

$$p_X(x) = \frac{1}{\sqrt{2\pi}}\exp\left[-\frac{u^2(x)}{2}\right]\frac{\mathrm{d}u(x)}{\mathrm{d}x}, \tag{7}$$

$$u(x) = [\sqrt{\xi^2(x) + c} + \xi(x)]^{1/3} - [\sqrt{\xi^2(x) + c} - \xi(x)]^{1/3} - a, \tag{8}$$

where

$$\xi(x) = 1.5b\left(a + \frac{x}{\alpha}\right) - a^3, \qquad a = \frac{\hat{h}_3}{3\hat{h}_4}, \quad b = \frac{1}{3\hat{h}_4}, \quad c = (b - 1 - a^2)^3,$$

$$\hat{h}_3 = \frac{\gamma_3}{4 + 2\sqrt{1 + 1.5\gamma_4}}, \qquad \hat{h}_4 = \frac{\sqrt{1 + 1.5\gamma_4} - 1}{18}, \qquad \alpha = \frac{1}{\sqrt{1 + 2\hat{h}_3^2 + 6\hat{h}_4^2}},$$

and γ_3 and γ_4 are the skewness and kurtosis of the fluctuating process, which reduce to zero for Gaussian.

An improvement to this model is suggested by using the expressions for $\hat{h}_3$ and $\hat{h}_4$ given previously (which are approximations) as initial conditions for solving the following pair of non-linear algebraic equations [5]:

$$\gamma_3 = \alpha^3(8\hat{h}_3^3 + 108\hat{h}_3\hat{h}_4^2 + 36\hat{h}_3\hat{h}_4 + 6\hat{h}_3), \tag{9}$$

$$\gamma_4 + 3 = \alpha^4(60\hat{h}_3^4 + 3348\hat{h}_4^4 + 2232\hat{h}_3^2\hat{h}_4^2 + 60\hat{h}_3^2 + 252\hat{h}_4^2 + 1296\hat{h}_4^3 + 576\hat{h}_3^2\hat{h}_4 + 24\hat{h}_4 + 3). \tag{10}$$

These equations have been derived by setting the third- and fourth-order central moments of $g[u(t)]$ equal to the known central moments of $x(t)$. This yields new coefficient values which exactly match the statistics up to the fourth order of the

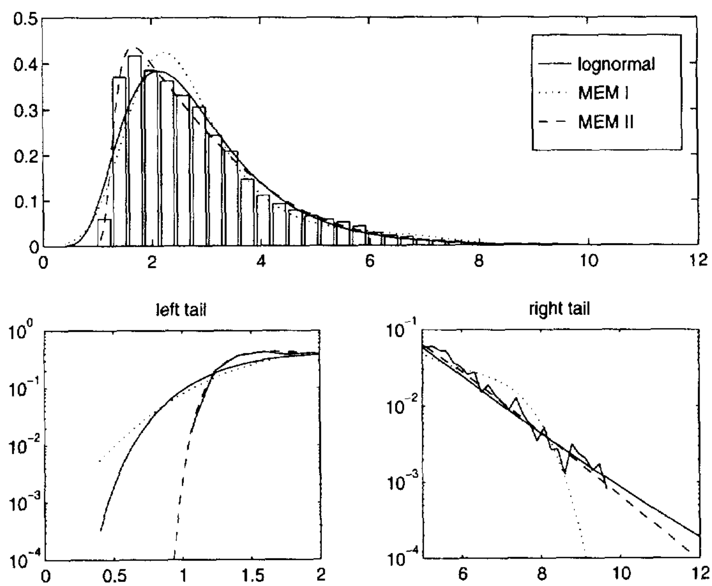

Fig. 1. Pressure data, MEP I, MEP II, and log-normal pdf estimates.

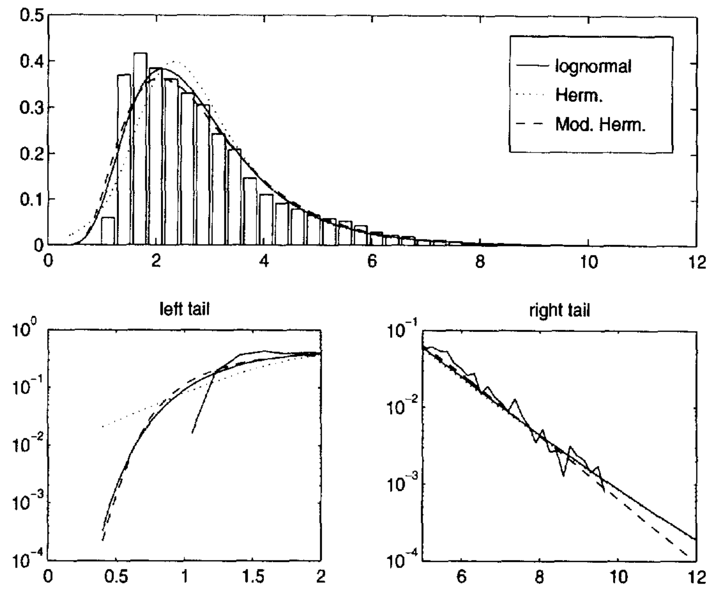

Fig. 2. Pressure data, Hermite, modified Hermite, and log-normal pdf estimates.

modeled non-Gaussian process. This is referred to herein as the modified Hermite method.

The transformation above is for the case when $x(t)$ is a softening process, e.g. the response of a linear system subjected to wind loads. A transformation for the case in which $x(t)$ is a hardening process is also available in the literature [4].

2.3. Pdf estimate example

Fig. 1 is the histogram of a measured pressure record, a log-normal fit, and two MEM fits. The MEM I fit demonstrates poor behavior in the tail, while the MEM II fit shows excellent consistency with the histogram in the mean as well as both tail regions. In this example the MEM II fit uses constraints in the form of $E[x]$, $E[x^{-2}]$, $E[x^{-3}]$, $E[x^{-4}]$.

Fig. 2 compares the same pressure data with a log-normal fit and standard and modified Hermite fits. Both the log-normal and modified Hermite fits are acceptable, while the standard Hermite fit gives a poor estimate in the left tail region. Chi-squared goodness of fit tests confirmed these observations.

Fig. 3 shows the data from a different pressure record and the pdf estimates using normal, log-normal, and modified Hermite estimates. A Chi-square test places the modified Hermite estimate within a 5% significance level, and the log-normal estimate well outside that range.

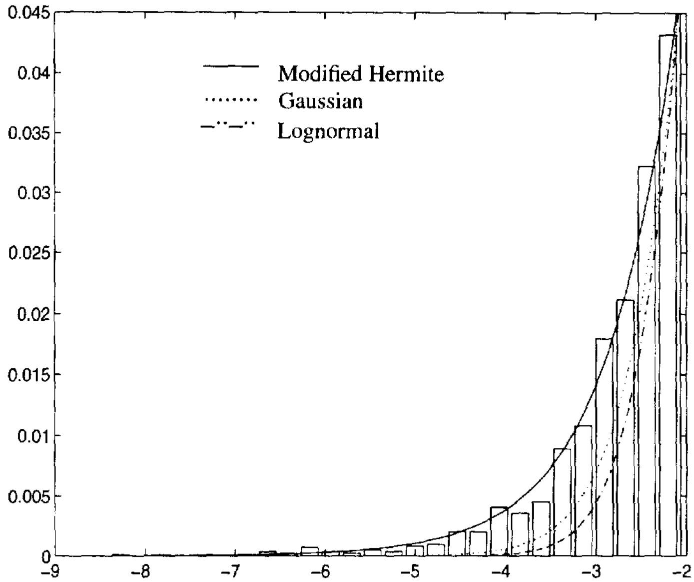

Fig. 3. Pressure data, Gaussian fit, log-normal fit, and modified Hermite fit.

3. Simulation of non-Gaussian pressure using static transformation

Among a host of techniques developed for the analysis and prediction of non-linear structural response, simulation methods are gaining popularity as computational efficiency increases. Implementation of time domain methods require simulated load time histories with case-specific statistical and spectral characteristics. When the assumption of Gaussian wind loading is inappropriate, e.g. cladding components and glass panels, techniques for simulating non-Gaussian loading must be sought. A method with wide utility will allow the user to specify non-Gaussian statistical parameters and the frequency content of the desired process.

3.1. Modified direct simulation with Hermite polynomials

An earlier study [6] presents the development of the so-called modified direct transformation for the simulation of non-Gaussian processes. This work focussed on the simulation of processes for which a sample is available, and is not capable of simulation based on a target spectrum and pdf. A non-Gaussian process is transformed to Gaussian using an iterative Hermite transformation which optimizes the transformation parameters to produce signal with Gaussian skewness and kurtosis. The power spectrum of this underlying Gaussian process is used to simulate independent Gaussian realizations, which are then transformed back to the non-Gaussian domain as independent realizations of the original signal. The modified direct simulation method is of limited use, as a sample signal is not always available during the design process as a basis for simulation. Further, the method is restricted to the non-Gaussian parameters and frequency content present in the sample. Next we consider a method which overcomes these shortcomings.

3.2. Spectral correction simulation

Spectral correction is a new method developed for simulation which is far more robust than the modified direct method. The user specifies non-Gaussian characteristics and frequency content in the form of the desired first four moments and a target power spectrum, respectively. The target moments and power spectrum may be based on measurements from a sample process, or derived through analytical means. Alternatively, the user may choose to define non-Gaussian characteristics through an analytical pdf.

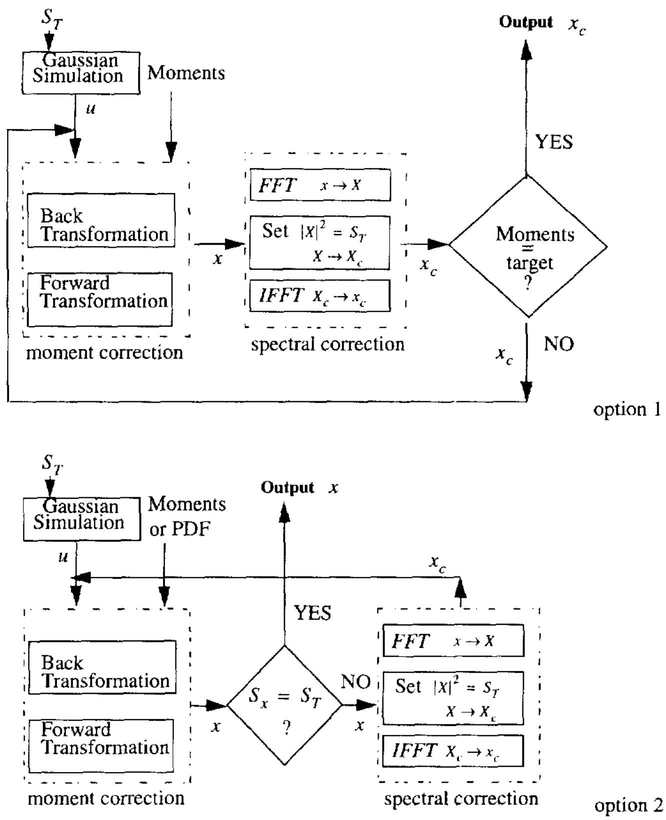

Fig. 4. Schematic of the spectral correction method, options one and two.

A schematic of the method is shown in Fig. 4, and uses both a moment correction and spectral correction transformation. Following option 1 (the top schematic in Fig. 4), the target spectrum S_{T} is used to produce a Gaussian process u. u is sent through a moment correction transformation, consisting of a back transformation to yield a Gaussian process u_g, then a forward transformation to yield a process x which matches the desired higher moments. The non-Gaussian process x has a power spectrum S_x which no longer matches the target spectrum S_{T}. The process x is sent through a spectral correction to produce x_c which fits the target spectrum S_{T}, and maintains the phase in x. The spectral correction transformation from x to x_c distorts the target moments in x. Thus, the second iteration begins by sending x_c back to the top of the loop to the moment correction.

The iterations continue until either the distorted moments of x_c converge to the target moments within a set tolerance after the spectral correction transformation (option 1), or the distorted spectrum converges to the target spectrum within a set tolerance after the moment correction transformation (option 2). When option 1 is chosen, the spectrum of the resulting simulated process will always match the target, and the higher moments will be within user-specified tolerance. When option 2 is chosen, the moments will match the target, and the spectrum will be within a specified tolerance. In option 2, the moment correction section of the iteration may be replaced with a cdf-type transformation [3], giving the user the option of describing the non-Gaussian characteristics of the desired process with either the first four moments, or an analytical pdf. This provides further motivation for the accurate modeling of pdfs presented in Section 2.

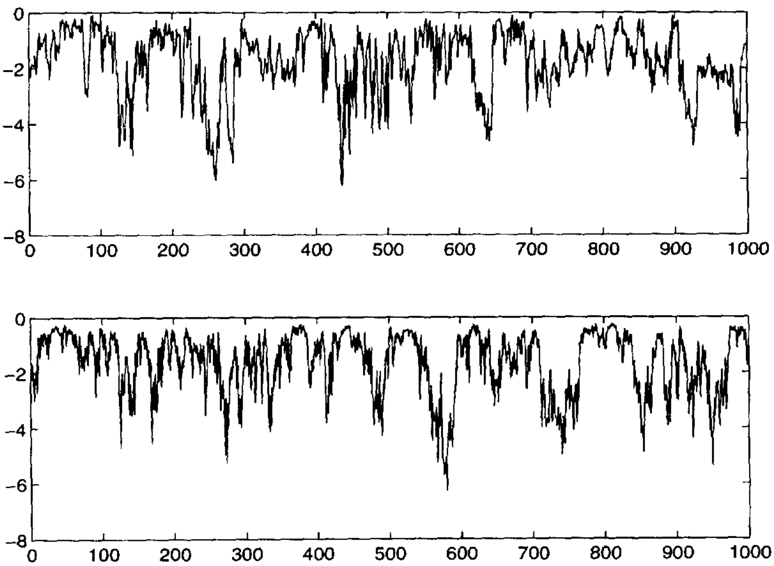

Fig. 5. A measured pressure record (top); spectral correction simulation (bottom).

3.3. Simulation example

An example uses the spectral correction method to simulate the measured pressure trace used previously. This is a practical example of a highly non-Gaussian process which is encountered in wind engineering. The spectral correction method matches the target power spectrum, with skewness and kurtosis within a user-specified error. The measured data has skewness and kurtosis values of -1.39 and 5.17, while the resulting simulation has corresponding values of -1.36 and 5.08, respectively. A portion of the measured pressure data and a realization using spectral correction are shown in Fig. 5. The characteristics of the target signal (e.g. occurrence rate, magnitude and grouping of extremes) are well represented in the simulation. The spectral correction method has recently been extended to multivariate and conditional non-Gaussian simulation [7].

4. Wavelet transform applications to stationary and non-stationary data

All the frequency domain techniques thus-far discussed contain the assumption of stationary behavior. Some pressure data under consideration in this study exhibits non-stationary or transient behavior, and requires methods to extract otherwise hidden information. The inability of conventional Fourier analysis tools to preserve the time dependence and describe the evolutionary spectral characteristics on non-stationary processes requires tools which allow time and frequency localization beyond customary Fourier analysis. One type of local transform is the recently developed discrete wavelet transform (DWT). Various dilations and translations of a parent wavelet are joined to form a family of basis functions which permit the retention of local signal characteristics beyond the capabilities of the harmonic basis functions. The dilations and translations of the parent wavelet are represented by the wavelet coefficients, analogous to the Fourier coefficients. The wavelet coefficients lend themselves to the analysis and simulation of the non-stationary pressure data through a variety of techniques, several of these methods are demonstrated by example in this study.

4.1. Scalogram

The local character of the wavelet coefficients provides the scalogram, which is a view of the coefficients on the time and frequency axis, and facilitates the identification of time-frequency energy flux and spectral evolution. The scalogram has been applied to the performance monitoring of structures with great success, e.g. distinguishing response due to impulsive-type loading events from large steady-state input, the identification of structural degradation, and the occurrence of non-ductile events.

Wavelet analysis of hurricane wind time histories, which contain significant contributions from convective turbulence, provides useful information regarding the distribution of energy content as a function of time. The response of a slender structure to wind may contain contributions from the fundamental mode and any number of higher modes depending on how the turbulent structure of the wind changes in time. The relative contribution of each mode may vary significantly or total building response may suddenly increase for apparently the same mean wind speed due to instantaneous changes in the distribution of energy at different frequencies. Such a response behavior cannot be identified through classical spectral techniques, while wavelet analysis is ideal for such an analysis.

As an example, 600 ft tall 100 ft square building is modeled with five degrees of freedom, and subjected to high (100 ft/s at 30 ft) wind as correlated point loads along its face. Fig. 6 is a scalogram of the response at the top floor of the building for two input cases. The scalogram, using Daubechies eighth-order wavelets, plots energy with respect to time (x-axis) and scale (y-axis), where the scales are marked as levels. The levels 1–5 are five frequency bands, with level 1 containing energy from one half

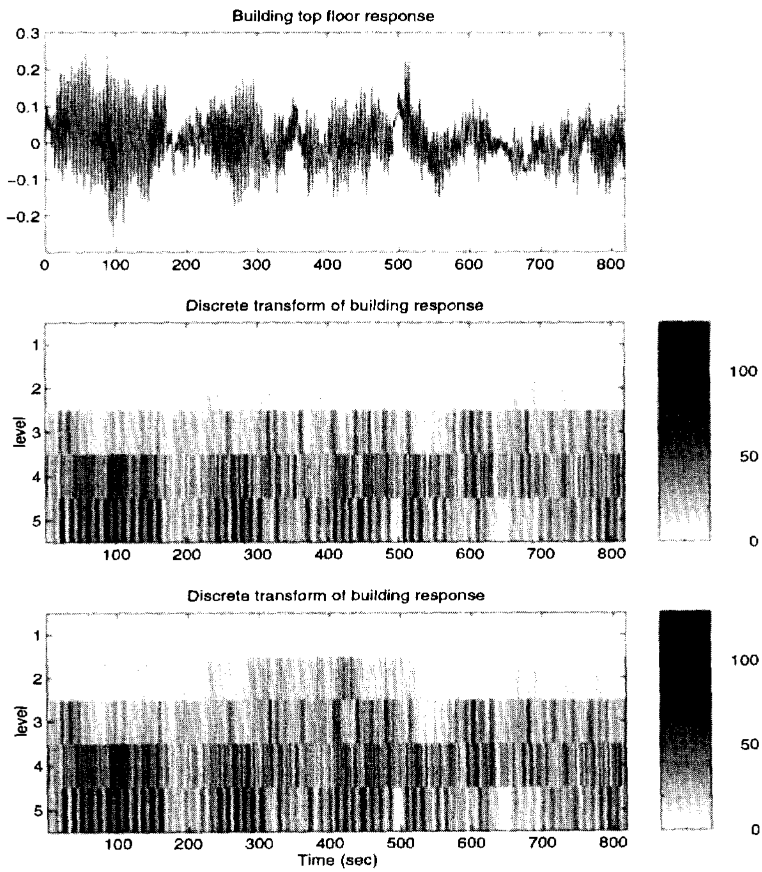

Fig. 6. Top floor building response to hurricane wind (top), scalogram of top floor response to stationary wind (middle), and scalogram of top floor response to wind with transient high-frequency fluctuations (bottom).

the cutoff frequency up to the cutoff. Level 2 contains energy from $\frac{1}{4}$ to $\frac{1}{2}$ of cutoff, and so on. Levels 2–5 contain all five modes of building response, with the fundamental mode in the fifth level, the second mode in the fourth level, and third and fourth modes in level 3, and the highest mode in level 2. The middle picture in Fig. 6 shows the response when the wind input is stationary, and the top plot is the response at the fifth floor for this input. The fundamental mode is represented by the darkest band seen in the fifth level, while the fifth mode at level 2 is hardly visible. The bottom picture is the top floor response when the wind input contains a transient burst of high-frequency fluctuations which stimulates the fifth mode for a short duration, visible as level 2 darkens then lightens with time. The response with transient energy in the fifth mode is indistinguishable from the response to stationary wind using Fourier methods or viewing the time histories, while the wavelet transformation clearly brings out the transient characteristics.

A very instructive potential application of wavelet decomposition on measured data can be seen in Ref. [8], addressing the response behavior of a bridge due to vortex shedding. In their paper the authors have noted that spectral methods of data analysis are not very helpful due to non-stationarity of the measured data. Also, to understand the behavior of the system the transition between regular and large amplitude response needs to be investigated. The spectral methods with constant bandwidth schemes do not permit zooming in time without losing resolution in frequency. Their investigation of response analysis can be best obtained through wavelet analysis as their data suggest changes in turbulence intensity and switching of response from one mode of oscillation to another during their measurements. Gurley and Kareem [7] have tried to overcome the shortcomings of the spectral approach by decomposing energy into different structural modes. We have demonstrated the effectiveness of wavelet-based analysis on this data in Ref. [9]. Wavelet analysis can serve as a more flexible tool for analyzing full-scale data with non-stationary features.

Intermittency of certain wavelengths in the approach flow may very well also explain unusual pressure fluctuations observed in full scale. These can be clearly identified using wavelet analysis [9].

4.2. Simulation

The retention of both time and frequency information makes wavelets a useful tool for the simulation of non-stationary signals. The simulation of non-stationary data may be done using either a sample non-stationary record directly, or a target spectrum and family of modulating functions. A non-stationary wind velocity record is decomposed using wavelet transforms to define a bank of envelope functions which describe signal modulation in time with respect to the desired frequency bands. This bank of modulators is then used to produce a new set of wavelet coefficients. A stochastic manipulation of these coefficients provides a realization statistically similar in both time and frequency characteristics to the sample non-stationary velocity record. Fig. 7 shows a measured non-stationary wind velocity record, and a simulated realization using the wavelet transform. Statistical comparisons between the target and simulated records, including spectra, the first four moments, and the

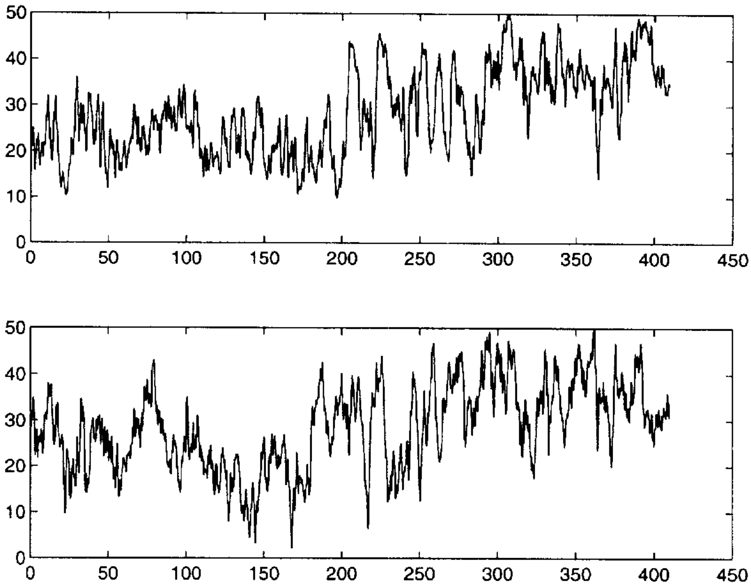

Fig. 7. Measured hurricane wind velocity record (top); wavelet simulation (bottom).

non-stationary trend in mean value are found to be good. A more detailed treatment will be included in a future publication.

5. Conclusions

This study presents several new methods for the modeling, analysis and simulation of non-Gaussian-measured wind and pressure records. Two new pdf models are based on earlier work using maximum entropy and Hermite transformation, and show potential for tremendous improvement over the commonly used log-normal distribution. An iterative method is presented for the simulation of highly non-Gaussian pressure given a target power spectrum and higher moments. Discrete wavelet transforms are used to delineate hidden information in the higher modes of response of a tall building in a wind storm like a hurricane wind field embedded with transient turbulent gusts of varying frequency content. Wavelets are also applied to the simulation of non-stationary wind velocity records. Examples are provided for each of the methods presented.

Acknowledgements

The support for this work was provided partially by ONR Grant N00014-93-1-0761, NSF Grant CMS95-03779, and a grant from Lockheed-Martin, INEL. The first author was partially supported by a Department of Education GAANNP fellowship.

References

[1] K. Sobczyk, J. Trebicki, Maximum entropy principle and nonlinear stochastic oscillators, Phys. A 193 (1993) 448–468.

[2] A. Kareem, J. Zhao, Analysis of non-Gaussian surge response of tension leg platforms under wind loads, J. Offshore Mech. Arctic Eng. ASME 116 (1994) 137–144.

[3] M. Grigoriu, Crossing of non-Gaussian translation process, J. Eng. Mech. ASCE 110 (4) (1984) 610–620.

[4] S.R. Winterstein, Nonlinear vibration models for extremes and fatigue, J. Eng. Mech. ASCE 114 (10) (1988) 1772–1790.

[5] M.A. Tognarelli, J. Zhoa, A. Kareem, Equivalent statistical cubicization: A frequency domain approach for nonlinearities in both system and forcing function, J. Eng. Mech. ASCE 123 (5) (1997).

[6] K. Gurley, A. Kareem, M. Tognarelli, Simulation of non-normal processes, Int. J. Nonlinear Mech. 31 (5) (1996) 601–617.

[7] K. Gurley, A. Kareem, Simulation of Correlated Non-Gaussian Pressure Fields, 2nd European and African Conf. on Wind Engineering, 2 EACWE, Genova, Italy, June 1997.

[8] J.S. Owen, A.M. Vann, J.P. Davies, A. Blakeborough, The prototype testing of Kessock Bridge: response to vortex shedding, J. Wind Eng. Ind. Aerodyn. 60 (1996) 91–106.

[9] K. Gurley, A. Kareem, Application of wavelet transforms in signal characterization, Department of Civil Engineering and Geological Sciences, Technical Report No. NDCE 96-004, Engineering Structures, 1996, submitted.